JOURNAL OF MAGNETIC RESONANCE **128,** 82–86 (1997)
ARTICLE NO. MN971208

The Effect of Magnetic Field Inhomogeneity on the Transverse Relaxation of Quadrupolar Nuclei Measured by Multiple Quantum Filtered NMR

U. Eliav,* T. Kushnir,† T. Knubovets,* Y. Itzchak,† and G. Navon*

**School of Chemistry, Tel Aviv University, Tel Aviv, Israel; and †Diagnostic Imaging Department, MRI Institute, The Chaim Sheba Medical Center, Tel Hashomer, Israel*

Received April 23, 1997

The effects of magnetic fields B_0 and B_1 inhomogeneities on techniques which are commonly used for the measurements of triple-quantum-filtered (TQF) NMR spectroscopy of ^{23}Na in biological tissues are analyzed. The results of measurements by pulse sequences with and without refocusing of B_0 inhomogeneities are compared. It is shown that without refocusing the errors in the measurement of the transverse relaxation times by TQF NMR spectroscopy may be as large as 100%, and thus, refocusing of magnetic field inhomogeneity is mandatory. Theoretical calculations demonstrate that without refocusing B_0 inhomogeneities the spectral width and phase depend on the interpulse time intervals, thus, leading to errors in the measured relaxation times. It is shown that pulse sequences that were used for the refocusing of the magnetic field (B_0) inhomogeneity also reduce the sensitivity of the experimental results to radiofrequency (B_1) magnetic field inhomogeneity.

In recent years there has been an increase in the application of surface coils to *in vivo* multiple quantum filtered (MQF) NMR spectroscopy of humans and animals (*1, 2*). Since for such coils the RF magnetic field (B_1) is very inhomogeneous, it is impossible to obtain hard pulses with a tilt angle of 180°, and thus magnetic field (B_0) inhomogeneities cannot be refocused. Refocusing of field inhomogeneities can be achieved without the use of 180° pulse by selecting a coherence pathway that results in an echo (*3–5*). In this study various pulse sequences with and without refocusing of field inhomogeneities are compared. It is shown that without refocusing the errors in the measurement of the transverse relaxation times by MQF spectroscopy may be as large as 100% and, thus, refocusing of magnetic field inhomogeneity is mandatory.

The system chosen for this study is 150 m*M* sodium chloride dissolved in 5% agarose gel. The transverse relaxation times of ^{23}Na were calculated from the triple quantum filtered (TQF) spectra. Figure 1 shows the pathway diagrams for the TQF pulse sequences with and without refocusing of the magnetic field inhomogeneity. Refocusing is accomplished either by a 180° pulse in the middle of the creation time in the standard TQF sequence (Fig. 1a) (*6*) or by selecting a pathway (Fig. 1e) in which equal time evolution of $p = 1$ and $p = -1$ coherences results in an echo (*5*).

We have compared the values obtained by the use of the TQF pulse sequence (Fig. 1a) with the full phase cycling of 192 steps (*7, 8*) to those determined from the TQF sequence without the 180° pulse and with various pathways (Figs. 1b–1e).

For pulse sequences a–d (Fig. 1) the dependence of the TQF spectra intensities on the creation time, τ, were analyzed in terms of a difference of two exponentials

$$f_{13}(\tau) \propto e^{-\tau/T_{2s}} - e^{-\tau/T_{2f}}, \qquad [1]$$

giving two transverse relaxation times, T_{2f} and T_{2s}.

For the pulse sequence e (Fig. 1), proposed by Kemp-Harper *et al.* (*5*), the transverse relaxation times were obtained by fitting the integrals of the TQF spectra to the expression

$$\int S(\tau/2, \omega_2)d\omega_2 \propto (e^{-\tau/2T_{2s}} - e^{-\tau/2T_{2f}})^2, \qquad [2]$$

where $S(\tau/2, \omega_2)$ are the TQF spectra.

The TQF experiments were conducted at various field inhomogeneities. The determination of the line broadening due to magnetic field inhomogeneity from the linewidth is cumbersome and not accurate. Since the lineshape is a superposition of two Lorentzians, one must subtract from the experimental spectrum a computed lineshape which is based on T_{2s} and T_{2f}. This procedure is unreliable particularly in cases where the contribution of the inhomogeneities is not large compared to the natural linewidth. Thus we estimated the magnetic field inhomogeneity by measuring the triple quantum relaxation time. The improved accuracy of this method is due to two reasons: (a) the contribution of the

1090-7807/97 $25.00

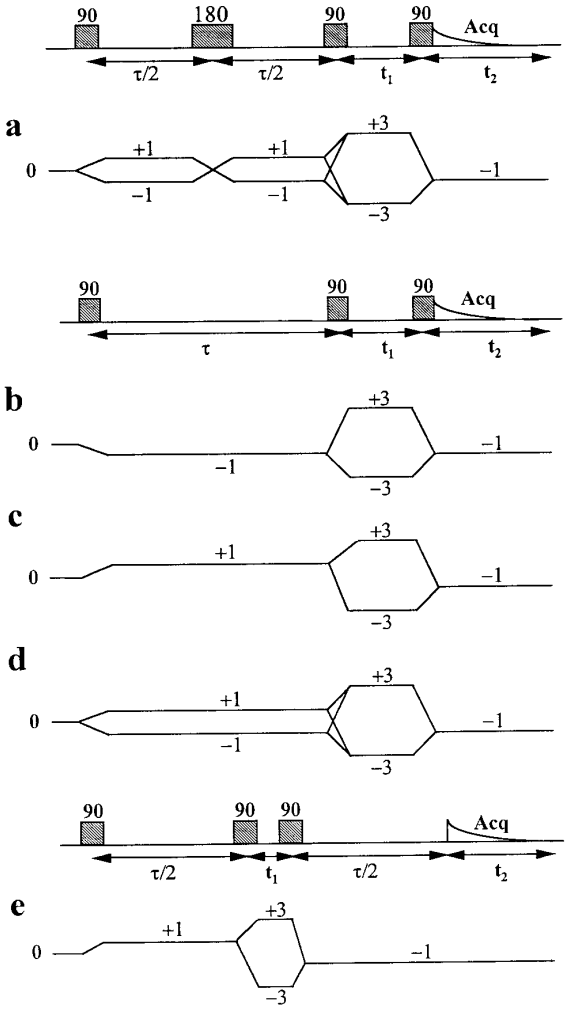

FIG. 1. Pathway selection diagrams: (a) $0 \rightarrow \pm 1 \rightarrow \pm 1 \rightarrow \pm 3 \rightarrow -1$ (with 180° refocusing pulse, pathway a); (b) $0 \rightarrow -1 \rightarrow \pm 3 \rightarrow -1$ (pathway b); (c) $0 \rightarrow +1 \rightarrow \pm 3 \rightarrow -1$ (pathway c); (d) $0 \rightarrow \pm 1 \rightarrow \pm 3 \rightarrow -1$ (pathways b + c, pathway d); (e) $0 \rightarrow +1 \rightarrow \pm 3 \rightarrow -1$ (the pulse sequence, proposed by Kemp-Harper *et al.* (*4*), pathway e).

magnetic field inhomogeneities to the triple quantum relaxation rate, $1/T_{TQ}^{*}$, is three times greater than that for the single quantum relaxation rate; (b) the natural relaxation, $1/T_{TQ}$, is relatively small and practically equal to T_{2s} (*6*, *9*). T_{TQ}^{*} is measured by monitoring the decay of the intensities of the standard TQF pulse sequence (Fig. 1a) spectra as a function of t_1. T_{TQ} was measured by the same pulse sequence but with a 180° pulse in the middle of the t_1 period. One should note that implicit assumption in the derivation of $1/T_{TQ}^{*}$ that the B_0 inhomogeneity has a Lorentzian lineshape is a gross approximation. Therefore $1/T_{TQ}^{*}$ should be taken to be an approximate measure of the size of the B_0 inhomogeneity.

The measurements were carried out on a Bruker AMX360-WB spectrometer, operating at sodium NMR frequency of 95.26 MHz. Experiments were performed on a broadband 10-mm probe at room temperature.

TABLE 1

Dependence of Sodium Transverse Relaxation Times on Coherence Pathway Selection and Magnetic Field Inhomogeneity in the TQF Pulse Sequence

		$\Delta\nu_{1/2}$ (Hz)[a]			
		5		8	
Pathway[b]	Refocusing	T_{2f} (ms)	T_{2s} (ms)	T_{2f} (ms)	T_{2s} (ms)
a	+	5.5 (5.5)	33.5 (33.1)	5.5 (5.5)	34.7 (34.1)
b	−	4.6 (3.9)	21.1 (22.5)	2.7 (2.7)	23.5 (14.5)
c	−	8.5 (6.9)	20.9 (17.4)	12.2 (8.6)	14.5 (10.1)
d	−	6.3 (5.7)	19.9 (17.1)	7.9 (5.2)	18.5 (13.8)
e	+	5.5 (5.5)	33.9 (33.5)	5.5 (5.5)	34.3 (34.0)

[a] Line broadening due to field inhomogeneity.
[b] See Fig. 1.

The results of the ^{23}Na TQF NMR experiments are summarized in Table 1 and Fig. 2. The values in the Table 1 have been obtained by analyzing the experimental data after Fourier transform with exponential broadening of 5 and 50 Hz (the latter data are given in parentheses).

The two-pulse sequences that result in refocusing of magnetic field inhomogeneity (Fig. 1a and Fig. 1e) yielded practically the same values of T_{2f} and T_{2s}. However, all pulse sequences where the magnetic field inhomogeneities are not refocused gave significantly different values of T_{2f} and T_{2s}. All the three of them resulted in shortened values of T_{2s} (see Fig. 2), while T_{2f} was shortened (Fig. 2, pathway b) in pulse sequence b (Fig. 1b) and lengthened significantly

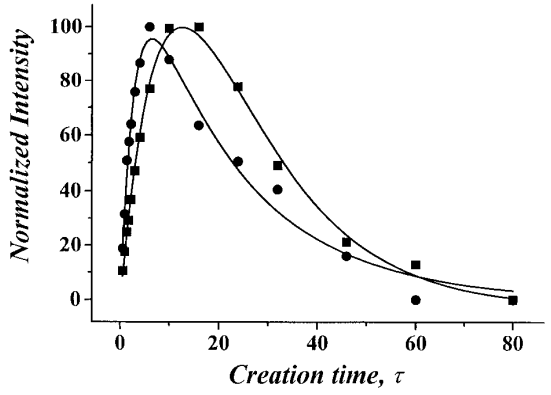

FIG. 2. Normalized ^{23}Na TQF NMR spectrum intensity for pathway b (Fig. 1b) (●) and pathway c (Fig. 1c) (■) as a function of the creation time, τ. Symbols correspond to the experimental data, while the lines are the curves fitted to Eq. [1].

(see Fig. 2, pathway c) in pulse sequences c and d (Figs. 1c and 1d).

In order to understand how the coherence pathways influence the deviations of the relaxation times from the correct values we have simulated the TQF intensities as a function of τ. The free induction decay for TQF pulse sequences is given by

$$\mathrm{FID}(\tau, t_2) = f_{13}(\tau) f_{13}(t_2) \int P(\omega_0) e^{-i\omega_0(t_2 - p\tau)} d\omega_0, \quad [3]$$

where $p = 0, -1, 1, 0$ for the pulse sequences a, b, c, and e (Fig. 1), respectively. The FID in pulse sequence d is the sum of the two pathways b and c. $P(\omega_0)$ is the function describing the magnetic field inhomogeneity. $P(\omega_0)$ was assumed to have either a symmetric ($\eta = 0.5$) (model 1) or an asymmetric ($\eta = 0.25$) (model 2) normalized Gaussian lineshape (Eq. [4]).

$$P(\omega_0) = \begin{cases} \omega_0 \leq 0 & \dfrac{1}{\Delta\omega_{1/2}\eta(1-\eta)} \sqrt{\dfrac{\ln 2}{4\pi}}\, e^{-(\omega_0/\eta\Delta\omega_{1/2})^2 \ln 2} \\ \omega_0 > 0 & \dfrac{1}{\Delta\omega_{1/2}\eta(1-\eta)} \sqrt{\dfrac{\ln 2}{4\pi}}\, e^{-(\omega_0/(1-\eta)\Delta\omega_{1/2})^2 \ln 2} \end{cases}, \quad [4]$$

where the variable ω_0 is the offset from the frequency of the peak of the distribution whose width at half height is $\Delta\omega_{1/2}$. The TQF spectra were calculated by Fourier transform of Eqs. [3] and [4]. In analogy to the way whereby the relaxation times are obtained from the experimental data, the peak intensities of the calculated TQF spectra were fitted to the expression given in Eq. [1] with T_{2f} and T_{2s} as free parameters. The resulting transverse relaxation times are given in Table 2. For comparison with the experimental data,

TABLE 2

Simulations of the Dependence of Transverse Relaxation Times on Coherence Pathway Selection and Magnetic Field Inhomogeneity ($\eta = 0.5$)

		$\Delta\nu_{1/2}$ (Hz)			
		8.3		20	
Pathway	Refocusing	T_{2f} (ms)	T_{2s} (ms)	T_{2f} (ms)	T_{2s} (ms)
a	+	5.6 (5.6)	32.6 (32.6)	5.6 (5.6)	32.6 (32.6)
b	−	6.4 (7.2)	15.4 (17.5)	6.2 (7.0)	6.3 (7.4)
c	−	7.9 (7.5)	27.6 (19.3)	13.8 (8.4)	14.6 (8.9)
d	−	6.5 (7.3)	23.6 (18.4)	7.9 (7.8)	18.3 (8.3)

TABLE 3

Simulations of the Dependence of Transverse Relaxation Times on Coherence Pathway Selection and Magnetic Field Inhomogeneity ($\eta = 0.25$)

		$\Delta\nu_{1/2}$ (Hz)			
		8.3		20.0	
Pathway	Refocusing	T_{2f} (ms)	T_{2s} (ms)	T_{2f} (ms)	T_{2s} (ms)
a	+	5.6 (5.6)	32.6 (32.6)	5.6 (5.6)	32.6 (32.6)
b	−	5.3 (6.8)	17.0 (16.0)	3.7 (4.0)	12.7 (11.1)
c	−	8.7 (8.0)	24.9 (16.3)	13.5 (7.8)	14.4 (8.5)
d	−	6.4 (7.3)	23.7 (16.3)	8.3 (6.3)	18.2 (9.4)

this procedure was done on spectra obtained from computed FID after exponential multiplication corresponding to line broadening of 5 and 50 Hz (the latter data are given in parentheses). As can be seen from Table 2, T_{2s} is longer when the magnetic field inhomogeneity is refocused. The values of T_{2f} for pathway c are longer than those for pathway b, in agreement with the experimental results (Table 1). However the simulated T_{2f} for pathway b is longer than the ''true'' value in the refocused sequences a and e in variance with the experimental results. This trend is reversed when an asymmetric Gaussian lineshape for the inhomogeneity is assumed (model 2, see Table 3). In the case of negligible field inhomogeneity or when the field inhomogeneity is refocused (pulse sequences a and e) exponential multiplication of the FID does not have any effect on the derived relaxation times. This is seen in both experimental and simulated results (Tables 1–3). When the field inhomogeneity is appreciable the derived relaxation times are sensitive to the choice of line broadening parameter, LB. The dependence of the derived relaxation times on the exponential multiplication may serve as an indication for lack of refocusing of the field inhomogeneity and reduced reliability of the derived relaxation times. The simulated effects of the exponential multiplication do not reproduce quantitatively the experimental results. However, we have noted that the combination of field inhomogeneity and a large value of LB causes the curve of the TQF spectra intensities as a function of τ to deviate from biexponential behavior.

The different dependence of the two pathways (Figs. 1b and 1c) on the magnetic field inhomogeneity may be discerned from the explicit expression for the spectrum that can be derived for the model where the inhomogeneity is described by a symmetric Gaussian function (model 1).

In this case the FID takes the form

$$\mathrm{FID}(\tau, t_2) = f_{13}(\tau) f_{13}(t_2) e^{-[(t_2 - p\tau)\Delta\omega_{1/2}]^2/16 \ln 2}. \quad [5]$$

The spectrum is obtained by Fourier transform of Eq. [5] with respect to t_2:

$$S(\omega_2, \tau) = f_{13}(\tau) e^{-\tau^2 \Delta\omega_{1/2}^2/16 \ln 2} S(\omega_2)$$

$$S(\omega_2) = \frac{2\sqrt{\ln 2}}{\sqrt{\pi}\,\Delta\omega_{1/2}} \left\{ e^{(r_{2s}+i\omega_2)^2 4 \ln 2/\Delta\omega_{1/2}^2} \times \operatorname{erfc}\left(\frac{r_{2s} + i\omega_2}{\Delta\omega_{1/2}} 2\sqrt{\ln 2} \right) - e^{(r_{2f}+i\omega_2)^2 4 \ln 2/\Delta\omega_{1/2}^2} \times \operatorname{erfc}\left(\frac{r_{2f} + i\omega_2}{\Delta\omega_{1/2}} 2\sqrt{\ln 2} \right) \right\}$$

$$r_{2s} = \frac{1}{T_{2s}} - p\tau\Delta\omega_{1/2}^2/8 \ln 2$$

$$r_{2f} = \frac{1}{T_{2f}} - p\tau\Delta\omega_{1/2}^2/8 \ln 2. \qquad [6]$$

The different dependence of r_i on τ for different p values in Eq. [6] is the origin of the different relaxation times obtained for pathways b ($p = -1$) and c ($p = +1$). Furthermore, from Eq. [6] one can conclude that the lineshape of $S(\omega_2)$ will change with the creation time, τ. It becomes narrower with increasing τ for $p = 1$ and broader for $p = -1$. The spectral linewidths are smaller than those obtained by the pulse sequences a and e (Fig. 1) for $p = 1$ while larger for $p = -1$. A phase distortion is also anticipated. An analogous situation of τ-dependent lineshapes occurs in anisotropic systems (*10, 11*). The common reason for these two apparently different cases is that in both the interactions that cause the line broadening, i.e., the field inhomogeneity in the present case and the residual quadrupolar interaction in the case of anisotropic systems, are not refocused. However, these two situations can be readily distinguished by using pulse sequence such as a or e (Fig. 1), where Zeeman interaction is refocused. Expressions similar to Eq. [6], that were derived for higher spins ($I > \frac{3}{2}$), (U. Eliav *et al.*, unpublished results) also show that the effect of the field inhomogeneity on the MQF lineshapes depends on the absolute value of the coherence as well as on its sign. This explains the results of Einarsson *et al.* (*12*) for ^{133}Cs ($I = \frac{7}{2}$) in DNA solutions that show dependence of linewidths of the MQ spectra on the coherences' absolute values and signs.

Another important aspect of the magnetic field inhomogeneity is its effect on the TQF signal sensitivity. In Table 4 the ratio between the maximum intensity of the TQF spectra for pulse sequences b, c, d, and e (Fig. 1) to that for the pulse sequence a (Fig. 1) is given as a function of the magnetic field inhomogeneity, $\Delta\omega_{1/2}$. The last row lists the theoretical values expected in the absence of inhomogeneity. It is interesting to note that while the peak intensity obtained using pathway 1b was smaller (50% of the standard TQF (Fig. 1a)), that obtained using pathway 1c was larger than the theoretical value. This effect can be understood by inspecting Eq. [6]. The effect of the inhomogeneity $\Delta\omega_{1/2}$ on r_i depends on the sign of the coherence p. In the refocusing pulse sequences, the second term ($-p\tau\Delta\omega_{1/2}^2$) in the expression for r_{2i} vanishes. Thus, relative to these sequences $\Delta\omega_{1/2}$ causes the value of r_{2i} to either decrease or increase for $p = 1$ or -1, respectively.

TABLE 4
The Maximum Intensity of the TQF Spectra Relative to That of Pulse Sequence a

	Pathway			
$\Delta\nu_{1/2}$ (Hz)	1b	1c	1d	1e
5	0.38	0.6	1	0.55
8	0.36	0.78	0.88	0.79
0	0.5	0.5	1	0.5

For the pulse sequence e (Fig. 1) a simple expression for the dependence of the spectral peak amplitude on τ is obtained if the lineshape of the field inhomogeneity is assumed to be a Lorentzian:

$$(e^{-\tau/2T_{2s}} - e^{-\tau/2T_{2f}})(T_{2s}^* e^{-\tau/2T_{2s}} - T_{2f}^* e^{-\tau/2T_{2f}}) \qquad [7]$$

where

$$1/T_{2s}^* = 1/T_{2s} + \Delta\omega_{1/2}/2 \quad 1/T_{2f}^* = 1/T_{2f} + \Delta\omega_{1/2}/2.$$

The advantage of the pulse sequence e (Fig. 1) lies in its low sensitivity to moderate B_1 inhomogeneities (*13*). However, since the dependence of the peak heights on τ (Eq. [7]) depends on the B_0 field inhomogeneity one cannot calculate T_{2s} or T_{2f} from such plot but rather from the peak integrals (Eq. [2]) that may be affected by baseline distortions.

The inhomogeneity has a larger effect in diminishing the peak intensity in the pulse sequence a than that in e. This can be easily verified by considering the limiting case where $\Delta\omega_{1/2} \gg 2/T_{2f}$. Under this condition the peak intensities for the pulse sequence e (Fig. 1) are proportional to $1/\Delta\omega_{1/2}$ (see Eq. [7]). On the other hand the peak height of pulse sequence a (Fig. 1) can be approximated by

$$(e^{-\tau/T_{2s}} - e^{-\tau/T_{2f}})(T_{2s}^* - T_{2f}^*), \qquad [8]$$

and thus under the above limiting condition of very large inhomogeneity the peak height is proportional to $1/\Delta\omega_{1/2}^2$ while for pulse sequence e (Fig. 1) it depends on the B_0 inhomogeneity as $1/\Delta\omega_{1/2}$. This explains our experimental

results that in the presence of field inhomogeneity the ratio between peak intensities in pulse sequences e and a (Fig. 1) exceeds the theoretical value of 0.5 (see Table 4).

We have also estimated the effect of B_1 inhomogeneity on the values of T_{2f} and T_{2s} in the case of the pulse sequence a (Fig. 1). The latter was found to be not very sensitive to B_1 inhomogeneity provided that the full phase cycling (192 steps) is used. The full phase cycling retains the coherence pathway described in Fig. 1a, while the more standard phase cycling does not eliminate extraneous coherences that results in a complex multiexponential relaxation leading to incorrect derived relaxation times. For isotropic systems B_1 inhomogeneity is causing the signal intensity dependence on τ to change from biexponential decay to triexponential (*4, 5*):

$$f_{13}(\tau) \propto (1 - \alpha)\exp\left(-\frac{\tau}{T_{2s}}\right) + \alpha \exp\left(-\frac{\tau}{2}\left(\frac{1}{T_{2s}} + \frac{1}{T_{2f}}\right)\right) - \exp\left(-\frac{\tau}{T_{2f}}\right)$$

For example, upon a deviation of the 180° pulse by $\pm 30°$ α gets the value of 0.16, and fitting the curve to two exponentials leads to a deviation of 10% and 1% for T_{2f} and T_{2s}, respectively, from the values given in Table 1.

In conclusion:

(a) All pulse sequences that do not refocus magnetic field inhomogeneity (Figs. 1b–1d) lead to serious errors in the derived relaxation times, T_{2s} and T_{2f}.

(b) Pulse sequence e (Fig. 1) can be used when both B_1 and B_0 are moderately inhomogeneous. The intensity of the obtained peak is comparable with that for the standard pulse sequence 1a. However, the analysis of the spectra measured by pulse sequence 1e requires the use of integral intensities and, thus, is sensitive to baseline distortions.

(c) Pulse sequence a (Fig. 1) with the full phase cycling gives the correct result provided that B_1 is not too inhomogeneous.

REFERENCES

1. R. C. Lyon, J. Pekar, C. T. W. Moonen, and A. C. McLauchlin, *Magn. Reson. Med.* **18,** 80 (1991).
2. R. Reddy, L. Bolinger, M. Shinnar, E. Noyszewski, and J. S. Leigh, *Magn. Reson. Med.* **33,** 134 (1995).
3. I. Furo and B. Halle, *J. Magn. Reson.* **98,** 388 (1992).
4. U. Eliav and G. Navon, *J. Magn. Reson. A* **115,** 241 (1995).
5. R. Kemp-Harper, P. Styles, and S. Wimperis, *J. Magn. Reson. B* **109,** 223 (1995).
6. G. Jaccard, S. Wimperis, and G. Bodenhausen, *J. Chem. Phys.* **85,** 6282 (1986).
7. G. Bodenhausen, H. Kogler, and R. R. Ernst, *J. Magn. Reson.* **58,** 370 (1984).
8. C.-W. Chung and S. Wimperis, *J. Magn. Reson.* **88,** 440 (1990).
9. L. Werbelow and G. Pouzard, *J. Phys. Chem.* **85,** 3887 (1981).
10. U. Eliav and G. Navon, *J. Magn. Reson. B* **103,** 19 (1994).
11. Y. Sharf, U. Eliav, H. Shinar, and G. Navon, *J. Magn. Reson. B* **107,** 60 (1995).
12. L. Einarsson, J. Kowalewski, L. Nordenskiöld, and A. Rupprecht, *J. Magn. Reson.* **85,** 228 (1989).
13. R. Kemp-Harper, P. Styles, S. P. Brown, C. E. Hughes, and S. Wimperis, *Prog. Magn. Reson.,* in press.